This article is published as part of the *Dalton Transactions* themed issue entitled:

Molecular Magnets

Guest Editor Euan Brechin
University of Edinburgh, UK

Published in issue 20, 2010 of *Dalton Transactions*

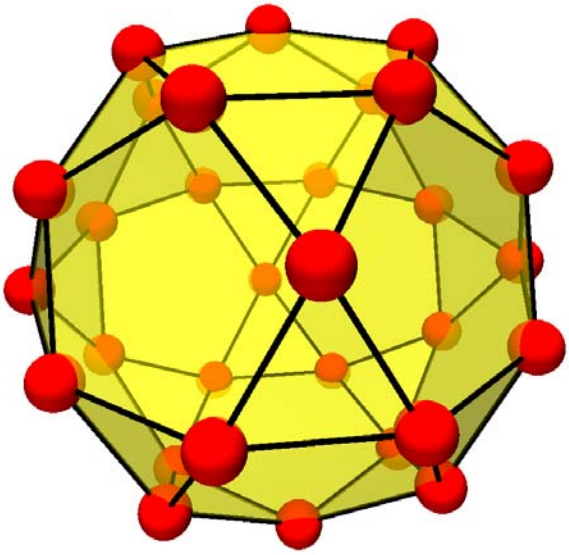

Image reproduced with permission of Jürgen Schnack

Articles in the issue include:

PERSPECTIVES:

COMMUNICATIONS:

A Mn_{15} single-molecule magnet consisting of a supertetrahedron incorporated in a loop†

Eleni E. Moushi,[a] Antonio Masello,[b] Wolfgang Wernsdorfer,[c] Vassilios Nastopoulos,[d] George Christou[b] and Anastasios J. Tasiopoulos*[a]

Received 4th January 2010, Accepted 14th April 2010
First published as an Advance Article on the web 26th April 2010
DOI: 10.1039/b927205d

Two new Mn_{15} clusters consisting of a supertetrahedron which is incorporated in a loop are reported. The reactions of $[Mn(O_2CEt)_2]\cdot 2H_2O$ with the diols 1,3-propanediol (H_2pd) or 2-methyl-1,3-propanediol (H_2mpd) in the presence of KX (X = CN^-, Cl^-, Br^-, NO_3^-, ClO_4^-, OCN^-, SCN^-) afforded compounds $[Mn_{15}K(\mu_4\text{-}O)_4(O_2CEt)_{11}(pd)_{12}(py)_2]$ (**1**) and $[Mn_{15}K(\mu_4\text{-}O)_4(O_2CEt)_{11}(mpd)_{12}(py)_2]$ (**2**). The structural core of **1** and **2** consists of a Mn_{11} loop and a Mn_9K supertetrahedron sharing a Mn_5 triangle. To the best of our knowledge, the structural motif of a supertetrahedron incorporated in a loop appears for the first time in metal cluster chemistry. Variable-temperature, solid-state direct current (dc) magnetic susceptibility studies in the 300–5 K range showed that the $\chi_M T$ value increases with decreasing T suggesting the existence of predominant ferromagnetic exchange interactions and a relatively large ground state spin. This was confirmed by field-variable temperature magnetization measurements which were fitted using a matrix diagonalization method to give $S \sim 23/2$, $g = 1.92(1)$ and $D = -0.071(2)$ cm^{-1}. In addition, compound **1** displays frequency-dependent alternating current (ac) signals suggesting single-molecule magnetism (SMM) behaviour. This was proven by magnetization *vs.* dc field sweeps on single-crystals of **1·0.7py·1.3MeCN**, which displayed sweep rate- and temperature-dependent hysteresis loops.

1. Introduction

Polynuclear Mn clusters continue to attract significant attention mainly due to their aesthetically pleasing structures and also their relevance to many areas including bioinorganic chemistry and materials science.[1,2] In the bioinorganic area, a number of Mn carboxylate clusters have been prepared to model the Mn_4 complex that is present in the active site of photosystem II and is responsible for the light-driven oxidation of water to molecular O_2.[1] The interest from the materials science point of view has been stimulated by the discovery that $[Mn_{12}O_{12}(O_2CMe)_{16}(H_2O)_4]$ can function as a single domain magnetic particle at low temperatures, displaying magnetization hysteresis and quantum tunneling of the magnetization (QTM).[2] This discovery initiated the field of molecular nanomagnetism, and such molecules have since been termed single-molecule magnets (SMMs).[2] A SMM derives its properties from a combination of a large ground state spin (S) value and an Ising (easy-axis) type of magnetoanisotropy (negative zero-field splitting parameter, D), which results in a barrier to magnetization relaxation. The upper limit of the latter is given by $S^2|D|$ and $(S^2 - 1/4)|D|$ for integer and half-integer spin systems, respectively. Although a number of SMMs have been prepared with a variety of paramagnetic metal ions,[3] manganese chemistry is still the most fruitful source of SMMs since polynuclear manganese complexes containing Mn^{3+} ions often combine large S values, with large (and negative) D values associated with the presence of Jahn–Teller distorted Mn^{3+} ions.[2] For this reason, significant efforts by groups all over the world, have been directed during the last few years towards the development of new synthetic routes to Mn clusters.[4–12] These efforts have resulted in important achievements in Mn cluster chemistry, including: (i) the synthesis of metal clusters with large nuclearities, up to 84, and novel structural topologies,[5,10] (ii) clusters that display large and sometimes abnormally large ground spin states, currently up to $83/2$[6,11a] and (iii) SMMs with large thermodynamic barriers (U) and large effective (kinetic) barriers (U_{eff}) to magnetization reversal.[7] Although several classes of Mn SMMs are now known,[2,4,5a,c,d,6c,7–9,11a] there is a continuing need for new types of such molecules to improve our understanding of this phenomenon.

Our group, has been exploring over the last few years the use of 1,3-propanediol (H_2pd) and 2-methyl-1,3-propanediol (H_2mpd) in Mn carboxylate chemistry as a route to new polynuclear clusters and SMMs. These ligands combine very promising features for Mn cluster chemistry, mainly due to the ability of their two hard RO^- groups to stabilize the hard Mn^{3+} ions and also to bridge two, three or four metal ions leading to high nuclearity metal clusters with a variety of structural cores. These studies have resulted in a number of new polynuclear clusters, including a family of 3-D coordination polymers consisting of Mn_{19} repeating units,[9] a $Mn_{40}Na_4$ loop of loops aggregate,[10] a metal cluster and two multidimensional

[a]*Department of Chemistry, University of Cyprus, 1678, Nicosia, Cyprus. E-mail: atasio@ucy.ac.cy; Fax: ++357 22892801; Tel: ++357 22892765*
[b]*Department of Chemistry, University of Florida, Gainesville, FL, 32611-7200, USA*
[c]*Institut Néel, CNRS/UJF, BP 166, Grenoble, Cedex 9, France*
[d]*Department of Chemistry, University of Patras, 26500, Patras, Greece*

† Electronic supplementary information (ESI) available: Plot of the out-of-phase (χ''_M) ac magnetic susceptibility *versus* T for **1**·0.5py and structural figures and tables for **2**. CCDC reference numbers 758907 and 758908. For ESI and crystallographic data in CIF or other electronic format see DOI: 10.1039/b927205d

coordination polymers based on Mn_{17} octahedra with large spin ground states which in the case of the discrete cluster was found to be $S = 37$,[11] and Mn_8 rods.[12] Most of these clusters were isolated from reactions that were involving the use of various Na^+-containing salts together with H_2(m)pd ligands in the reaction mixtures, although only the first two compounds include Na^+ ions in their asymmetric units.

Herein we report an extension of these investigations towards the use of various K^+-containing salts together with H_2(m)pd ligands, which has led to compounds $[Mn_{15}K(\mu_4\text{-}O)_4(O_2CEt)_{11}(pd)_{12}(py)_2]$ (**1**) and $[Mn_{15}K(\mu_4\text{-}O)_4(O_2CEt)_{11}(mpd)_{12}(py)_2]$ (**2**). Both complexes consist of a supertetrahedron which is incorporated in a loop, a topology which to the best of our knowledge appears for the first time in cluster chemistry. Furthermore, compound **1** has a large ground spin state of $S = 23/2$ and displays hysteresis loops in magnetization *versus* applied direct current (dc) magnetic field scans and is thus a new SMM.

Experimental

Syntheses

All manipulations were performed under aerobic conditions using materials (reagent grade) and solvents as received; water was distilled in-house. $Mn(O_2CEt)_2{\cdot}2H_2O$[13] was synthesized according to a published method. Elemental analyses (C, H, N) were performed by the in-house facilities of the University of Florida, Chemistry Department.

$[Mn_{15}K(\mu_4\text{-}O)_4(O_2CEt)_{11}(pd)_{12}(py)_2]$ (1)

Method A. To a solution of $[Mn(O_2CEt)_2]{\cdot}2H_2O$ (0.131 g, 0.55 mmol) in a 10 : 2 ml mixture of MeCN/py was added H_2pd (0.20 ml, 2.77 mmol) and KCN (0.036 g, 0.55 mmol). The resulting yellowish–brown slurry was then left under magnetic stirring for about sixteen hours. It was then filtered, and the filtrate was left undisturbed at room temperature. After a few days X-ray quality crystals of **1·0.7py·1.3MeCN** appeared and were collected by filtration, washed with MeCN and dried in vacuum. The yield was ~ 39%. Elemental analysis: (%) calcd for $C_{81.5}H_{139.5}N_{2.5}O_{50}KMn_{15}$ (**1·0.5py**): C 34.74, H 4.99, N 1.24, Found: C 34.73, H 4.76, N 1.25. Selected IR data (KBr): $\tilde{\nu}$ = 3435(s, br), 2941(w), 2853(w), 1589(w), 1414(w), 1298(w), 1094(s), 947(w), 833(w), 669(w), 604(s), 527(w).

Method B. Method A was repeated using various K^+-containing salts such as KCl, KBr, KNO_3, $KClO_4$, KOCN or KSCN in place of KCN. The yields were ~25%–35%. The products were identified by IR spectral comparison with authentic material and from unit cell determination.

$[Mn_{15}K(\mu_4\text{-}O)_4(O_2CEt)_{11}(mpd)_{12}(py)_2]$ (2)

Complex **2** was prepared by following a similar procedure to the one described above with the only difference being the use of H_2mpd instead of H_2pd. The yield was ~34%. Elemental analysis: (%) calcd for $C_{96}H_{166}N_3O_{50}KMn_{15}$ (**2**·py): C 38.11, H 5.53, N 1.39, Found: C 37.84, H 5.44, N 1.19. Selected IR data (KBr): $\tilde{\nu}$ = 3424(s, br), 2902(w), 2858(w), 1618(s), 1404(s), 1300(w), 1105(m), 1059(m), 627(s), 486(w).

Table 1 Crystallographic data for complexes [**1**·0.7py·1.3MeCN] and [**2**·1.1py·0.7MeCN]

	[**1**·0.7py·1.3MeCN]	[**2**·1.1py·0.7MeCN]
Formula[a]	$C_{85.10}H_{144.40}KMn_{15}N_4O_{50}$	$C_{97.90}H_{168.60}KMn_{15}N_{3.80}O_{50}$
Mw	2886.85	3062.17
Crystal System	Triclinic	Triclinic
Space group	$P\bar{1}$	$P\bar{1}$
a/Å	14.1453(6)	16.7239(4)
b/Å	20.7559(7)	20.9456(6)
c/Å	21.378(1)	21.7298(6)
α/°	107.132(4)	61.502(3)
β/°	102.343(4)	81.995(2)
γ/°	93.518(3)	87.622(2)
V/Å^3	5807.3(4)	6621.6(3)
Z	2	2
T/K	100(2)	100(2)
λ[b]/Å	0.71073	0.71073
D_c/g cm^{-3}	1.651	1.536
μ(Mo Kα)/mm^{-1}	1.692	1.488
Reflections collected	78 946	23 200
Obs. refl. [$I > 2\sigma(I)$]	9394	14106
R_{int}	0.070	0
R_1%[c]	0.0443	0.0722
wR_2[d]	0.0805	0.2074
Goodness of fit on F^2	0.930	1.049
$\Delta\rho$max/min/e Å^{-3}	1.196/−0.520	1.314/−0.849

[a] Including solvent molecules. [b] Graphite monochromator. [c] $R_1 = \sum\|F_o| - |F_c\|/\sum|F_o|$. [d] $wR_2 = [\sum[w(F_o^2 - F_c^2)^2]/\sum[wF_o^2)^2]]^{1/2}$, $w = 1/[\sigma^2(F_o^2) + (m{\cdot}p)^2 + n{\cdot}p]$, $p = [\max(F_o^2,0) + 2F_c^2]/3$, and m and n are constants.

X-Ray crystallography†

Data were collected on an Oxford-Diffraction Xcalibur diffractometer, equipped with a CCD area detector and a graphite monochromator utilizing Mo-Kα radiation (λ = 0.71073 Å). Suitable crystals were attached to glass fibers using paratone-N oil and transferred to a goniostat where they were cooled for data collection. Unit cell dimensions were determined and refined by using 15 190 ($3.01 \leq \theta \leq 30.53°$) and 21 799 ($3.04 \leq \theta \leq 30.28°$) reflections for **1**·0.7py·1.3MeCN and **2**·1.1py·0.7MeCN respectively. Empirical absorption corrections (multi-scan based on symmetry-related measurements) were applied using CrysAlis RED software.[14] The structures were solved by direct methods using SIR92,[15a] and refined on F^2 using full-matrix least squares using SHELXL97.[15b] Software packages used: CrysAlis CCD[14] for data collection, CrysAlis RED[14] for cell refinement and data reduction, WINGX for geometric calculations,[15c] and DIAMOND[16a] and MERCURY[16b] for molecular graphics. The non-H atoms were treated anisotropically, whereas the hydrogen atoms were placed in calculated, ideal positions and refined as riding on their respective carbon atoms. Unit cell data and structure refinement details are listed in Table 1. Full details can be found in the CIF files provided in the ESI.†

Physical measurements

IR spectra were recorded on KBr pellets in the 4000–400 cm^{-1} range using a Shimadzu Prestige-21 spectrometer. Variable-temperature DC magnetic susceptibility data down to 1.80 K were

collected on a Quantum Design MPMS-XL SQUID magnetometer equipped with a 70 kG (7 T) DC magnet at the University of Florida. Diamagnetic corrections were applied to the observed paramagnetic susceptibilities using Pascal's constants. Samples were embedded in solid eicosane, unless otherwise stated, to prevent torquing. AC magnetic susceptibility data were collected on the same instrument, employing a 3.5 G field oscillating at frequencies up to 997 Hz. Magnetization *vs.* field and temperature data were fit using the program MAGNET.[17] Studies at ultra-low temperatures (<1.8 K) were performed on single crystals at Grenoble using an array of micro-SQUIDs.[18] The high sensitivity of this magnetometer allows the study of single crystals of the order of 10 to 500 μm; the field can be applied in any direction by separately driving three orthogonal coils.

Results and discussion

Syntheses

As was mentioned above, our group has been investigating the use of the H_2pd and H_2mpd ligands in Mn carboxylate chemistry. During these investigations we have widely employed various Na^+-containing salts in the Mn/H_2(m)pd reaction mixtures. These investigations were expanded to the systematic study of the use of a combination of various Na^+-containing salts and H_2(m)pd ligands in Mn carboxylate chemistry, after the isolation of two new 3-D coordination polymers based on the $[Mn_{19}Na(\mu_4\text{-}O)_9(\mu_3\text{-}O)(\mu_3\text{-}OH)_3(O_2CMe)_9(L)_9(H_2O)_3](OH)$ (L = pd^{2-}, mpd^{2-}) repeating unit.[9] The results of these studies were a large $[Mn_{40}Na_4(\mu_3\text{-}O)_8(O_2CMe)_{52}(pd)_{24}(py)_8]$ loop consisting of four Mn_{10} loops linked through Na^+ ions[10] and also numerous other compounds which do not contain Na^+ ions in their asymmetric unit.[11,12] An obvious extension of these investigations involved the use of various K^+-containing salts in Mn/H_2(m)pd chemistry. These experiments resulted in a new family of Mn_{15} clusters consisting of a supertetrahedron incorporated in a loop. Thus, the reaction of $[Mn(O_2CEt)_2]\cdot 2H_2O$ with H_2pd and KCN in a 1 : 5 : 1 ratio in MeCN : py (10 : 2 ml) resulted in the formation of brown crystals of **1**·0.7py·1.3MeCN in ~39% yield. The choice of KCN as a K^+ source was made because it also contains CN^- groups that can act as both bridging and terminal ligands in Mn cluster chemistry.[19] However compound **1** does not contain neither coordinated nor lattice CN^- groups. In order, to determine whether KCN plays an additional role in this reaction apart from the provision of K^+ ions the same reaction was repeated with the use of other K^+-containing salts. Thus, compound **1** was also isolated in ~25–35% yields by following the same reaction procedure with the only difference being the use of KCl, KBr, KNO_3, $KClO_4$, KOCN or KSCN, instead of KCN. The analogous reaction, using H_2mpd instead of H_2pd was also performed, resulting in the formation of brown crystals of complex **2**·1.1py·0.7MeCN in 34% yield. Although all the reactions took place in organic solvents (MeCN/py), where some of the above mentioned K^+-containing salts are nearly insoluble, we should note that the solvents were used as received and contain small amounts of water; thus the K^+ - containing salts are slightly soluble in these solvent systems. The K^+-containing salt that dissolves reacts rapidly, more salt then dissolves and the colour of the reaction mixture changes to darker yellow-brown as the reaction proceeds. After ~16 h of magnetic stirring almost all the salt has reacted and the yellowish-brown slurry is filtered off. Crystals of **1**·0.7py·1.3MeCN and **2**·1.1py·0.7MeCN were formed when the filtrates were left undisturbed for a few days. Both complexes are mixed valent, containing Mn^{2+}, Mn^{3+} and Mn^{4+} ions. Note, that although we used a Mn^{2+}-containing starting material in the synthesis, the reaction products contain not only Mn^{2+} but also several Mn^{3+} and one Mn^{4+} ions; we believe that the $Mn^{3+/4+}$ ions were formed upon oxidation of the Mn^{2+} ions by atmospheric O_2, a process widely found in manganese chemistry.[12] The oxidation in this case was base-assisted, since the reaction solution contained a large amount of pyridine. The formation of compounds **1** and **2** is summarized in eqn (1) (L = pd^{2-} or mpd^{2-}).

$$15Mn(O_2CEt)_2 + 12H_2L + KCN + 2py + 3O_2 \rightarrow \mathbf{[Mn_{15}K(\mu_4\text{-}O)_4(O_2CEt)_{11}(L)_{12}(py)_2]} + 19EtCOOH + HCN + 2H_2O \quad (1)$$

Description of structures

The molecular structure of complex **1** is presented in Fig. 1 and selected interatomic distances are listed in Table 2. Bond valence sum (BVS) calculations for the metal ions of **1** are given in Table 3. The crystal structures of **1** and **2** present a striking similarity and thus only that of **1** will be described here; structural figures and tables with selected interatomic distances and BVS calculations for the metal ions of **2** are provided in the supporting information.†

Compound [**1**·0.7py·1.3MeCN] crystallizes in the triclinic $P\bar{1}$ space group. Its crystal structure reveals that **1** (Fig. 1) is a mixed valent complex that contains four Mn^{II}, ten Mn^{III} and one Mn^{IV} ions, as determined by bond valence sum (BVS) calculations (Table 3), charge considerations and inspection of metric parameters. All fifteen Mn ions are in a distorted octahedral

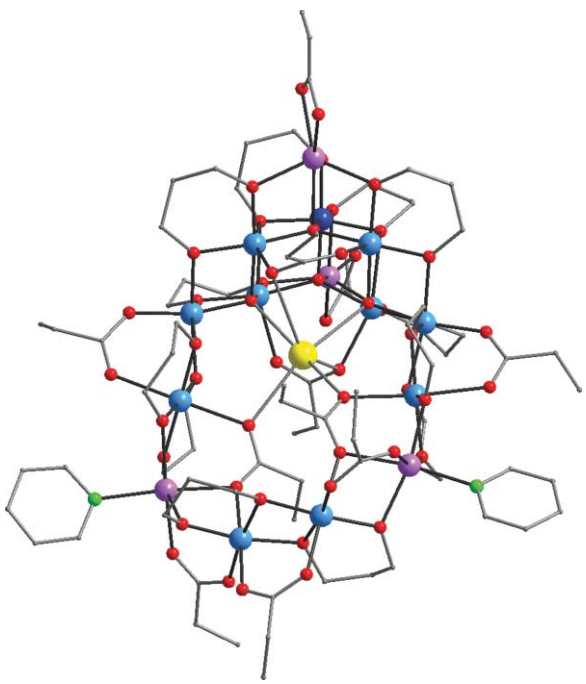

Fig. 1 Molecular structure of complex **1**. Colour code: Mn^{II}, purple; Mn^{III}, blue; Mn^{IV}, dark blue; K, yellow; O, red; N, green; C, grey. Hydrogen atoms have been omitted for clarity.

Table 2 Selected interatomic distances (Å) for complex **1**

K^{+}–O	2.695(3)–3.003(4)
Mn^{2+}–O	2.078(3)–2.346(3)
Mn^{3+}–O	1,862(3)–2.445(3)
Mn^{4+}–O	1.877(3)–1.910(3)
Mn^{2+}–N	2.222(5)–2.230(5)

Table 3 Bond valence sum (BVS)[a,b] calculations for complex **1**

	Mn^{II}	Mn^{III}	Mn^{IV}
Mn1	**1.94**	1.78	1.87
Mn2	4.25	3.89	**4.08**
Mn3	**1.90**	1.74	1.83
Mn4	3.25	**2.97**	3.12
Mn5	3.25	**2.98**	3.13
Mn6	3.24	**2.96**	3.11
Mn7	3.35	**3.06**	3.21
Mn8	3.19	**2.92**	3.06
Mn9	3.26	**2.98**	3.13
Mn10	**2.04**	1.94	2.00
Mn11	3.25	**2.97**	3.12
Mn12	3.29	**3.01**	3.16
Mn13	**2.02**	1.92	1.98
Mn14	3.28	**3.00**	3.15
Mn15	3.16	**2.89**	3.04

[a] The bold value is the one closest to the charge for which it was calculated. [b] The oxidation state is the nearest whole number to the bold value.

geometry with the ten Mn^{III} ions displaying the expected Jahn–Teller elongations, although these are not co-parallel. The core of **1** (Fig. 2) consists of a Mn_{11} loop (Fig. 2, bottom, right) and a Mn_9K supertetrahedron (Fig. 2, bottom, left) sharing a Mn_5 triangle. The eight Mn ions of the supertetrahedron are placed in two stacked isosceles triangles with the ninth one being in the apex position. Its base consists of four Mn^{III} ions and one Mn^{II} ion located at the corners and the edges of an isosceles triangle, and a K^+ lying ~1.38 Å from one of the sides of the triangle. The second triangle comprises of two Mn^{III} and one Mn^{IV} ions, whereas at the apex of the supertetrahedron is a Mn^{II} ion. The Mn_9K unit is held together by four μ_4-O^{2-} bridges resulting in a $[Mn^{IV}Mn^{III}{}_6Mn^{II}{}_2K^{I}O_4]^{19+}$ core (Fig. 2, bottom, left) that contains metal ions in oxidation states ranging from +1 to +4. The peripheral ligation of the supertetrahedron is completed by six pd^{2-} and four propionate ligands. The Mn_{11} loop consists of a Mn_6 semicircle and the Mn_5 basal triangle of the supertetrahedron described above (Fig. 2, bottom, right). The four Mn^{III} and two Mn^{II} ions of the semicircle are linked through five propionate and two pd^{2-} ligands and also one RO^- arm of four more pd^{2-}. The second arm of the latter and two propionate ligands connect the Mn_6 semicircle with the Mn_5 triangle. The peripheral ligation of the Mn_6 semicircle is completed by two terminal pyridine molecules. The Mn_{11} loop surrounds a K^+ ion which is connected to the Mn_{15} unit through two μ_4-O^{2-} ligands and four $O_{propionate}$ atoms (the K–O bond lengths range from 2.695(3)–3.003(4) Å) adopting a distorted octahedral geometry (Fig. 3, right).

All propanediol and propionate ligands are fully deprotonated as determined by BVS calculations, charge considerations and inspection of metric parameters. Ten pd^{2-} ligands bridge two Mn^{III} ions and one Mn^{II} ion in a η^2:η^2:μ_3 fashion whereas the remaining two bridge one Mn^{II}, two Mn^{III} and one Mn^{IV} ions in a η^2:η^3:μ_4 fashion (Fig. 3, left). In addition, nine of the $EtCOO^-$

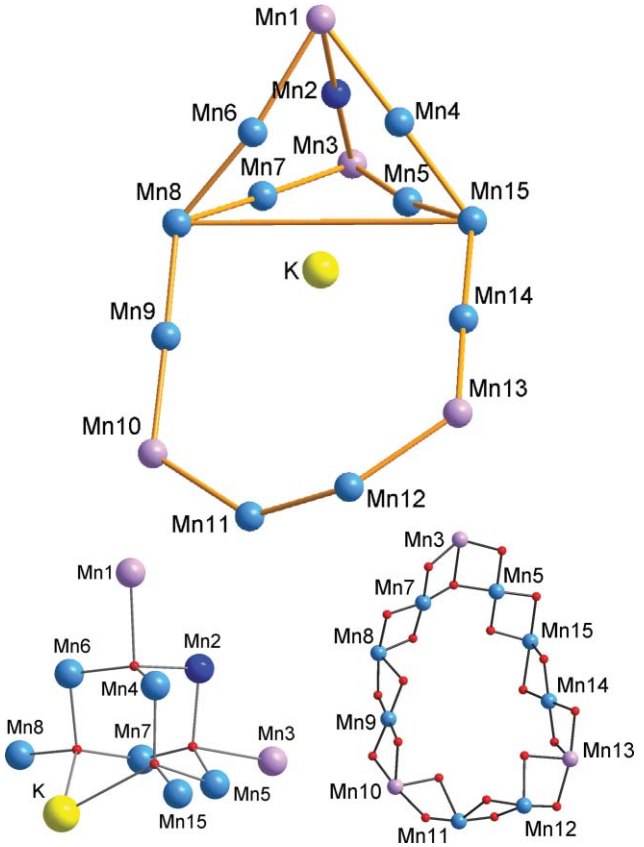

Fig. 2 Partially labelled representations of: (top) the metallic skeleton of complex **1** (the gold line connecting the Mn ions is to emphasize the topology of **1**), (bottom, left) the central manganese oxide core of the Mn_9K supertetrahedron and (bottom, right) the Mn–O core of the Mn_{11} loop. Colour code: Mn^{II}, purple; Mn^{III}, blue; Mn^{IV}, dark blue; K, yellow; O, red.

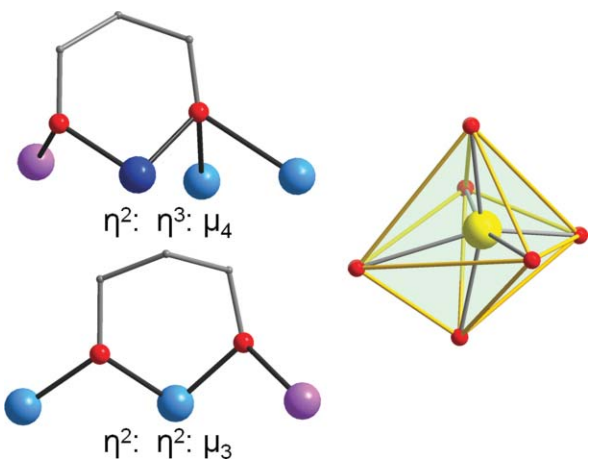

Fig. 3 Representations of: (left) the coordination modes of the pd^{2-} ligands and (right) the distorted octahedral geometry around the K^+ ion, of complex **1**. The gold line connecting the O atoms is to emphasize the octahedral topology of the K^+ ion. Colour code: Mn^{II}, purple; Mn^{III}, blue; Mn^{IV}, dark blue; K^+, yellow; O, red; C, grey.

ligands bridge in *syn*,*syn*-η^1:η^1:μ_2, η^2:η^1:μ_3 and η^2:η^2:μ_4 modes respectively and the remaining two act as bidentate chelates. A close examination of the packing of **1** reveals the parallel

alignment of the molecules. Although there are no significant intermolecular hydrogen-bonding interactions, the Mn_{15} aggregates are in relatively close proximity, since the shortest Mn $\cdots$ Mn separation between different Mn_{15} units is ~7.26 Å (Mn2 $\cdots$ Mn1′). As mentioned above, compound **2** is very similar to **1** with the main difference being the existence of mpd^{2-} ligand instead of pd^{2-}.

Compounds **1** and **2** join a very small family of pentadecanuclear Mn complexes,[20] and possess a structural topology that appears for the first time in metal cluster chemistry. In addition, their two sub-units also display interesting structural features. For example, the Mn_9K unit possesses a beautiful and unusual supertetrahedral structural core which has appeared only a few times before in Mn cluster chemistry.[21] Note that the Mn_9K core (Fig. 2, bottom, left) of **1** and **2** display significant differences compared to those of the known compounds including: (i) the existence of a heterometal (K) in the M_{10} units, (ii) a slightly different structural topology, associated with the presence of the K^+ ion which results in a significant distortion of the supertetrahedral topology and (iii) different oxidation states of the Mn ions, *etc.* In addition, the structural topology of the second sub-unit of **1** and **2**, *i.e.* the Mn_{11} loop, is unknown in discrete form. In fact, the isolation of a discrete Mn_{11} loop would be particularly attractive since it would be a very rare example of an odd numbered loop[22] and the first undecanuclear ring.

Magnetochemistry

Dc magnetic susceptibility studies

Solid-state, variable-temperature magnetic susceptibility measurements were performed on a vacuum-dried microcrystalline sample of **1**·0.5py, which was suspended in eicosane to prevent torquing. The dc magnetic susceptibility (χ_M) data were collected in the temperature range of 5.0–300 K, in a 0.1 T magnetic field and are plotted as $\chi_M T$ *vs.* T in Fig. 4. The $\chi_M T$ value at 300 K is 49.36 $cm^3\ mol^{-1}$ K and is almost equal to the spin-only ($g = 2$) value of 49.375 $cm^3\ mol^{-1}$ K expected for a [Mn_{15}] unit comprising four Mn^{II}, ten Mn^{III} and one Mn^{IV} non-interacting ions. The $\chi_M T$ value then increases gradually with decreasing temperature to a maximum of 60.09 $cm^3\ mol^{-1}$ K at 6.5 K, before decreasing to 59.18 $cm^3\ mol^{-1}$ K at 5.0 K. This behaviour is indicative of the existence of dominant ferromagnetic exchange interactions in **1**. In addition, the maximum of 60.09 $cm^3\ mol^{-1}$ K at 6.5 K suggests that **1** possesses a relatively large spin ground state value of $S = 21/2$ or $23/2$; the spin-only ($g = 2$) values for $S = 21/2$ and $23/2$ are 60.375 and 71.875 $cm^3\ mol^{-1}$ K, respectively. The small decrease at low temperatures (< 6.5 K) is likely due to zero-field splitting (ZFS), Zeeman effects from the applied field, and/or weak intermolecular interactions. Given the size of the Mn_{15} molecule and the resulting number of inequivalent exchange constants, it is not possible to apply the Kambe method to determine the individual pairwise exchange interaction parameters between the Mn ions, and direct matrix diagonalization methods are also computationally unfeasible.

To determine the ground state of **1**, magnetization (M) *versus* dc field measurements were made on restrained samples in the magnetic field (H) and temperature ranges of 1.8–10.0 K and 1.0–70.0 kG (0.1–7 T). The resulting data are shown in Fig. 5 as a reduced magnetization ($M/N\mu_\beta$) *versus* H/T plot, where N is Avogadro's number and μ_B is the Bohr magneton. The data were fit using the program MAGNET,[17] which assumes that only the ground state is populated at these temperatures, includes axial zero-field splitting ($D\hat{S}_z^2$) and isotropic Zeeman interactions with the applied field, and carries out a full powder average. The corresponding Hamiltonian is given by eqn (2)

$$H = D\hat{S}_z^2 + g\mu_B\mu_0\hat{S}H \quad (2)$$

where D is the axial anisotropy, $\hat{S}_z$ is the easy-axis spin operator, g is the electronic g factor, μ_0 is the vacuum permeability, and H is the applied field. However, we could not get an acceptable fit using data collected over the whole field range, which is a common problem caused by the existence of low-lying excited states or/and intermolecular interactions. As has been described elsewhere on multiple occasions for mixed valence Mn clusters[5c,6c,9,23] a common solution to this problem is to use only data collected at low fields. Indeed, a reasonable fit of the reduced magnetization data could be achieved when data collected in fields only up to 3 T were employed. The fit is shown as the solid line in Fig. 5 and the fit parameters were $S = 23/2$, $D = -0.071(2)$ cm^{-1} and $g = 1.92(1)$, slightly less than 2.0 as expected for mixed valent complexes

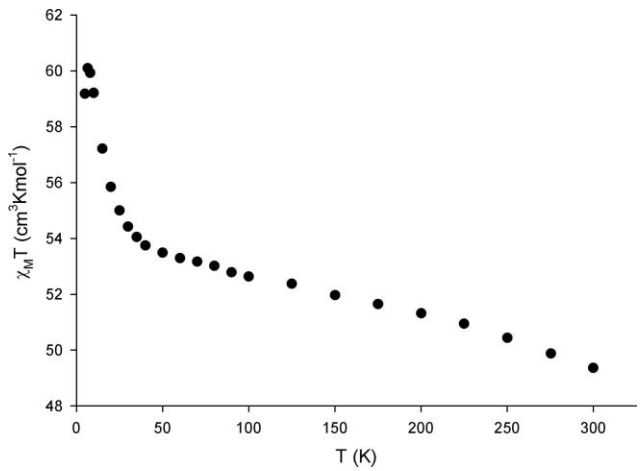

Fig. 4 Plot of $\chi_M T$ *vs.* T for **1**·0.5py.

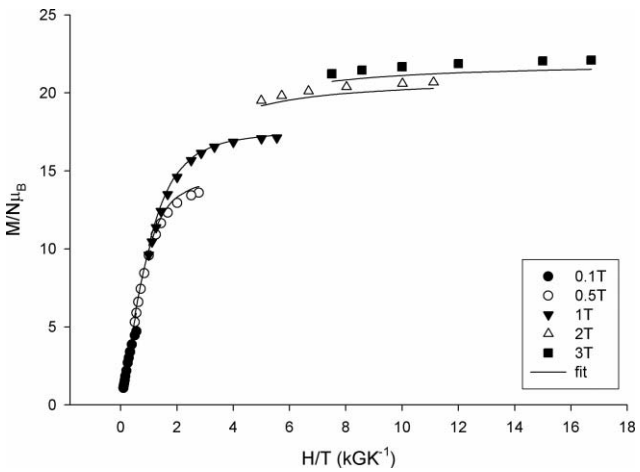

Fig. 5 Plot of reduced magnetization ($M/N\mu_\beta$) *vs.* H/T for **1**·0.5py at applied fields of 0.1–3.0 T and in the 1.8–10 K temperature range. The solid lines are the fit of the data. See text for details.

containing Mn^{III} and/or Mn^{IV} ions.[6c,19a,23a,b] Attempts were also made to fit the data assuming a $S = 21/2$ spin ground state, since this value was also suggested together with the $S = 23/2$ from the variable temperature dc magnetic susceptibility data; however the resulting fits were of poorer quality and gave too large g values (>2.04) for Mn clusters.

As has been described in the past,[5b,d,9-11,23] ac susceptibility studies provide a powerful complement to dc studies for determining the ground state of a system because they preclude any complications arising from the presence of a dc field. We thus carried out detailed ac studies on complex **1** in order to determine independently its ground state S and also to detect the slow magnetization relaxation suggestive of SMM behaviour.

Ac magnetic susceptibility studies

Alternating current susceptibility data were collected in the 1.8–15 K range using a 3.5 G ac field oscillating at frequencies in the 50–997 Hz range. If the magnetization vector can relax fast enough to keep up with the oscillating field, then there is no imaginary (out-of-phase) susceptibility signal (χ''_M), and the real (in-phase) susceptibility (χ'_M) is equal to the dc susceptibility. The $\chi'_M T$ extrapolated from a temperature high enough to avoid the effects of any weak intermolecular interactions or slow relaxation, to 0 K (where only the ground state would be populated) should thus be in agreement with $\chi'_M T = (g^2/8)S(S + 1)$ where S is the ground state of the compound. However, if the barrier to magnetization relaxation is significant compared to the thermal energy (kT), then χ'_M decreases and there is a non-zero χ''_M. Such frequency-dependent χ''_M signals are a characteristic signature of the superparamagnetic-like properties of a SMM.

For complex **1** the in-phase signal (χ'_M, plotted as $\chi'_M T$ *vs.* T, Fig. 6) increases slightly from ~61.3 at 15 K to ~65.3 cm^3 mol^{-1} K at 6 K and then decreases rapidly at temperatures lower than 6 K. The small increase of the $\chi'_M T$ values is most likely due to depopulation of excited states with spin S smaller than that of the ground state. The rapid decrease of the $\chi'_M T$ below ~6 K is due to the ZFS and weak intermolecular interactions. In addition, below ~2.8 K there is a frequency-dependent decrease in $\chi'_M T$ and a concomitant appearance of frequency-dependent χ''_M signals (electronic supplementary information†); only the beginnings of peaks appear above 1.8 K, the peak maxima clearly lying at lower temperatures. Extrapolation to 0 K of $\chi'_M T$ from values above 6 K, to avoid complications from effects such as intermolecular interactions and ZFS at lower temperatures gives a value of ~67.5 cm^3 mol^{-1} K, which indicates a ground spin state of $S = 23/2$ with g ~1.94, in satisfying agreement with the results of the dc magnetization fits above. In contrast, $S = 21/2$ ground state would be expected to give values of slightly less than 60.4 cm^3 mol^{-1} K, *i.e.* significantly smaller than the one obtained from the ac studies of **1**·0.5py. We now can return back in the variable temperature dc magnetic susceptibility studies and rationalize the small value (for a $S = 23/2$ system) of the maximum of 60.09 cm^3 mol^{-1} K at 6.5 K on the basis of the existence of populated low-lying excited states at this temperature and magnetic field with spin S smaller than that of the ground state in agreement with the conclusion from the ac magnetic susceptibility studies.

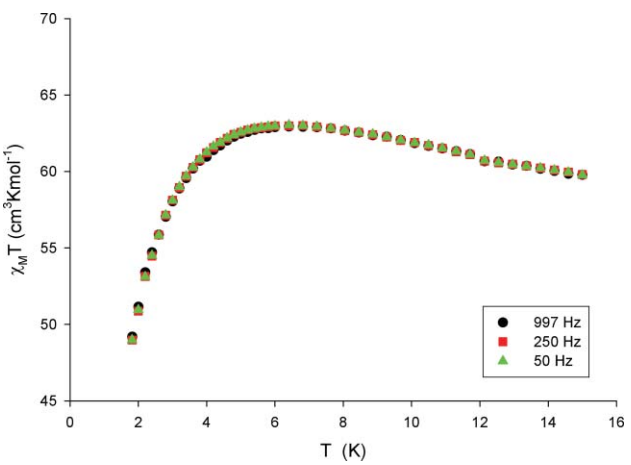

Fig. 6 Plot of the in-phase (χ'_M) (as $\chi'_M T$) ac magnetic susceptibility *versus* T for **1**·0.5py at the indicated frequencies.

Magnetization *versus* dc field hysteresis studies

The observation of out-of-phase ac signals suggested that **1** might be a new SMM, although such signals by themselves are not proof of a SMM.[10] To confirm whether **1** is indeed a SMM, magnetization *versus* dc field scans were carried out on a single crystal of **1**·0.7py·1.3MeCN using a micro-SQUID apparatus.[18] The obtained magnetization *versus* applied dc field responses are plotted in Fig. 7, showing both the temperature dependence at 0.017 T s^{-1} and the scan rate dependence at 0.04 K. Hysteresis loops were observed below ~0.6 K, whose coercivities increase with decreasing temperature and increasing field sweep rate, as expected for the superparamagnetic-like properties of a SMM. The data thus confirm complex **1**·0.7py·1.3MeCN to be a new addition to the family of SMMs, with a blocking temperature (T_B) of ~0.6 K, above which there is no hysteresis. The hysteresis loops contain a large step at zero field, which we assign to ground-state QTM through the anisotropy barrier *via* the lowest lying $M_S = \pm 23/2$ levels of the $S = 23/2$ manifold. In other parts of the hysteresis loops, there are no clear steps characteristic of QTM; this behaviour is typical for large SMMs, which are more susceptible to step-broadening effects associated with low-lying excited states, intermolecular interactions, and distributions of local environments due to ligand and solvent disorder.[5a,c,d,6c,8b,9,23c]

Magnetization *versus* time decay data were collected on a single crystal of **1**·0.7py·1.3MeCN in order to obtain a more quantitative assessment of the magnetization relaxation dynamics. The sample's magnetization was first saturated in one direction at ~5 K with a large applied dc field, the temperature was then decreased to a chosen value, and then the field was removed and the magnetization decay was monitored with time. The results are shown in Fig. 8 for the 0.04–0.6 K range. Attempts were made to calculate the relaxation rate at the different temperatures, to construct an Arrhenius plot and fit the data based on eqn (3)

$$\tau = \tau_0 \exp(U_{eff}/kT) \quad (3)$$

where τ_0 is the pre-exponential factor, U_{eff} is the effective relaxation barrier and k is the Boltzmann constant. However, we were unable to obtain a reasonable fitting most likely because **1**·0.7py·1.3MeCN does not follow the Arrhenius law, due to

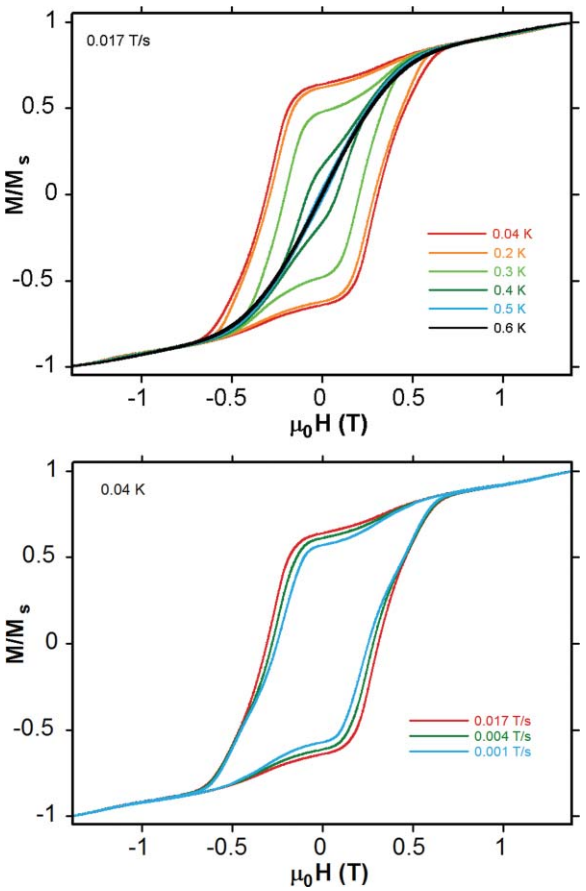

Fig. 7 Magnetization (M) *vs.* applied magnetic field ($\mu_0 H$) hysteresis loops for a single crystal of **1**·0.7py·1.3MeCN (top) at the indicated temperatures and a fixed field sweep rate of 0.017 T s^{-1} and (bottom) at the indicated field sweep rates and a constant temperature of 0.04 K. M is normalized to its saturation value, M_S.

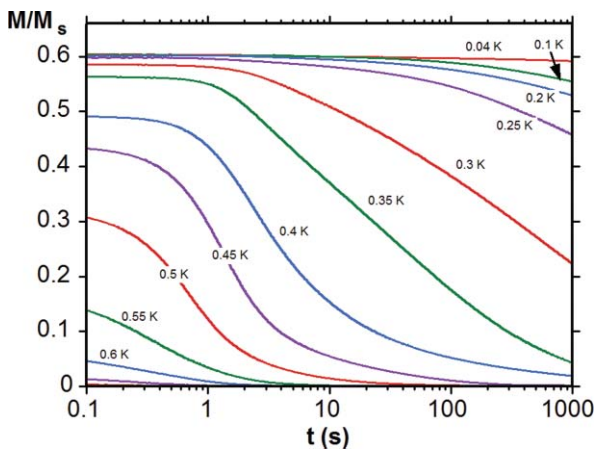

Fig. 8 Magnetization (M) *vs.* time decay plots in zero dc field for a single crystal of **1**·0.7py·1.3MeCN. The magnetization is normalized to its saturation value, M_S.

contributions to the relaxation rate of pathways *via* excited spin states as has also been recently reported to be the case for a series of other SMMs.[8a,b,24]

Conclusions

The present work provides a further confirmation of the ability of H_2pd and H_2mpd ligands to lead to beautiful polynuclear Mn clusters. So far, apart from **1** and **2**, the use of H_2pd and H_2mpd has resulted in four more families of Mn clusters some of which display large nuclearities, new structural topologies and interesting magnetic properties.[9-12] Compounds **1** and **2** were the initial results from an extension of our investigations to the use of various K^+-containing salts together with H_2pd and H_2mpd ligands in Mn carboxylate chemistry. The two Mn_{15} clusters consist of a supertetrahedron that is incorporated in a loop, a structural topology that appears for the first time in metal cluster chemistry. Magnetism studies revealed that **1** possesses a relatively large spin ground state of $S = 23/2$ and display SMM behaviour. Further studies on the use of M^{n+}-containing salts (M = alkali metal ion, $n = 1$; M = alkaline earth metal ion, $n = 2$) together with H_2pd and H_2mpd ligands are in progress and these results will be reported in due course.

Acknowledgements

This work was supported by the Cyprus Research Promotion Foundation (Grant: ΔΙΕΘΝΗΣ/ΣΤΟΧΟΣ/0308/14) and the USA National Science Foundation (CHE-0910472).

Notes and references

1 (*a*) J. Barber, *Chem. Soc. Rev.*, 2009, **38**, 185; (*b*) S. Mukhopadhyay, S. K. Mandal, S. Bhaduri and W. H. Armstrong, *Chem. Rev.*, 2004, **104**, 3981.
2 (*a*) R. Sessoli, H.-L. Tsai, A. R. Schake, S. Wang, J. B. Vincent, K. Folting, D. Gatteschi, G. Christou and D. N. Hendrickson, *J. Am. Chem. Soc.*, 1993, **115**, 1804; (*b*) G. Christou, D. Gatteschi, D. N. Hendrickson and R. Sessoli, *MRS Bull.*, 2000, **25**, 66; (*c*) R. Sessoli, D. Gatteschi, A. Ganeschi and M. A. Novak, *Nature*, 1993, **365**, 141; (*d*) R. Bagai and G. Christou, *Chem. Soc. Rev.*, 2009, **38**, 1011.
3 (*a*) H. Andres, R. Basler, A. J. Blake, C. Cadiou, G. Chaboussant, C. M. Grant, H. U. Güdel, M. Murrie, S. Parsons, C. Paulsen, F. Semadini, V. Villar, W. Wernsdorfer and R. E. P. Winpenny, *Chem.–Eur. J.*, 2002, **8**, 4867; (*b*) K. W. Galloway, A. M. Whyte, W. Wernsdorfer, J. Sanchez-Benitez, K. V. Kamenev, A. Parkin, R. D. Peacock and M. Murrie, *Inorg. Chem.*, 2008, **47**, 7438; (*c*) F. Klöwer, Y. Lan, J. Nehrkorn, O. Waldmann, C. E. Anson and A. K. Powell, *Chem.–Eur. J.*, 2009, **15**, 7413; (*d*) A. L. Barra, D. Gatteschi and R. Sessoli, *Chem.–Eur. J.*, 2000, **6**, 1608; (*e*) S. L. Castro, Z. Sun, C. M. Grant, J. C. Bollinger, D. N. Hendrickson and G. Christou, *J. Am. Chem. Soc.*, 1998, **120**, 2365; (*f*) P.-H. Lin, T. J. Burchell, R. Clérac and M. Murugesu, *Angew. Chem., Int. Ed.*, 2008, **47**, 8848.
4 (*a*) G. Christou, *Polyhedron*, 2005, **24**, 2065; (*b*) G. Aromi and E. K. Brechin, *Struct. Bond.*, **2006**, 1; (*c*) E. K. Brechin, *Chem. Commun.*, 2005, 5141; (*d*) A. J. Tasiopoulos and S. P. Perlepes, *Dalton Trans.*, 2008, 5537; (*e*) T. C. Stamatatos and G. Christou, *Inorg. Chem.*, 2009, **48**, 3308.
5 (*a*) A. J. Tasiopoulos, A. Vinslava, W. Wernsdorfer, K. A. Abboud and G. Christou, *Angew. Chem., Int. Ed.*, 2004, **43**, 2117; (*b*) R. T. W. Scott, S. Parsons, M. Murugesu, W. Wernsdorfer, G. Christou and E. K. Brechin, *Angew. Chem., Int. Ed.*, 2005, **44**, 6540; (*c*) M. Soler, W. Wernsdorfer, K. Folting, M. Pink and G. Christou, *J. Am. Chem. Soc.*, 2004, **126**, 2156; (*d*) T. C. Stamatatos, K. A. Abboud, W. Wernsdorfer and G. Christou, *Angew. Chem., Int. Ed.*, 2008, **47**, 6694.
6 (*a*) A. M. Ako, I. J. Hewitt, V. Mereacre, R. Clérac, W. Wernsdorfer, C. E. Anson and A. K. Powell, *Angew. Chem., Int. Ed.*, 2006, **45**, 4926; (*b*) C.-H. Ge, Z.-H. Ni, C.-M. Liu, A.-L. Cui, D.-Q. Zhang and H.-Z. Kou, *Inorg. Chem. Commun.*, 2008, **11**, 675; (*c*) T. C. Stamatatos, K. A. Abboud, W. Wernsdorfer and G. Christou, *Angew. Chem., Int. Ed.*, 2007, **46**, 884.
7 (*a*) C. J. Milios, A. Vinslava, W. Wernsdorfer, S. Moggach, S. Parsons, S. P. Perlepes, G. Christou and E. K. Brechin, *J. Am. Chem. Soc.*,

2007, **129**, 2754; (*b*) C. J. Milios, R. Inglis, A. Vinslava, R. Bagai, W. Wernsdorfer, S. Parsons, S. P. Perlepes, G. Christou and E. K. Brechin, *J. Am. Chem. Soc.*, 2007, **129**, 12505; (*c*) C. J. Milios, S. Piligkos and E. K. Brechin, *Dalton Trans.*, 2008, 1809.
8 (*a*) G. Karotsis, S. J. Teat, W. Wernsdorfer, S. Piligkos, S. J. Dalgarno and E. K. Brechin, *Angew. Chem., Int. Ed.*, 2009, **48**, 8285; (*b*) A. M. Ako, V. Mereacre, R. Clérac, W. Wernsdorfer, I. J. Hewitt, C. E. Anson and A. K. Powell, *Chem. Commun.*, 2009, 544; (*c*) S. Maheswaran, G. Chastanet, S. J. Teat, T. Mallah, R. Sessoli, W. Wernsdorfer and R. E. P. Winpenny, *Angew. Chem., Int. Ed.*, 2005, **44**, 5044; (*d*) D. J. Price, S. R. Batten, B. Moubaraki and K. S. Murray, *Chem. Commun.*, 2002, 762; (*e*) S. K. Langley, K. J. Berry, B. Moubaraki and K. S. Murray, *Dalton Trans.*, 2009, 973; (*f*) R. W. Saalfrank, A. Scheurer, R. Prakash, F. W. Heinemann, T. Nakajima, F. Hampel, R. Leppin, B. Pilawa, H. Rupp and P. Müller, *Inorg. Chem.*, 2007, **46**, 1586.
9 E. E. Moushi, T. C. Stamatatos, W. Wernsdorfer, V. Nastopoulos, G. Christou and A. J. Tasiopoulos, *Angew. Chem., Int. Ed.*, 2006, **45**, 7722.
10 E. E. Moushi, C. Lampropoulos, W. Wernsdorfer, V. Nastopoulos, G. Christou and A. J. Tasiopoulos, *Inorg. Chem.*, 2007, **46**, 3795.
11 (*a*) E. E. Moushi, T. C. Stamatatos, W. Wernsdorfer, V. Nastopoulos, G. Christou and A. J. Tasiopoulos, *Inorg. Chem.*, 2009, **48**, 5049; (*b*) E. E. Moushi, T. C. Stamatatos, V. Nastopoulos, G. Christou and A. J. Tasiopoulos, *Polyhedron*, 2009, **28**, 1814.
12 E. E. Moushi, T. C. Stamatatos, V. Nastopoulos, G. Christou and A. J. Tasiopoulos, *Polyhedron*, 2009, **28**, 3203.
13 T. Lis, *Acta Crystallogr., Sect. B: Struct. Crystallogr. Cryst. Chem.*, 1977, **33**, 2964.
14 Oxford Diffraction 2008, *CrysAlis CCD and CrysAlis RED*, version 1.171.32.15, Oxford Diffraction Ltd, Abingdon, Oxford, England.
15 (*a*) A. Altomare, G. Cascarano, C. Giaconazzo, A. Guagliardi, M. C. Burla, G. Polidori and M. Camalli, *SIR92, J. Appl. Crystallogr.*, 1994, **27**, 435; (*b*) G. M. Sheldrick, *SHELXL97*, University of Göttingen, Germany; (*c*) L. J. Farrugia, *J. Appl. Crystallogr.*, 1999, **32**, 837.
16 (*a*) K. Brandenburg, 2006, *DIAMOND*. Version 3.1d. Crystal Impact GbR, Bonn, Germany; (*b*) C. F. Macrae, P. R. Edgington, P. McCabe, E. Pidcock, G. P. Shields, R. Taylor, M. Towler and J. Van de Streek, *J. Appl. Crystallogr.*, 2006, **39**, 453.
17 E. R. Davidson, *MAGNET*, Indiana University: Bloomington, IN, 1999.
18 W. Wernsdorfer, *Adv. Chem. Phys.*, 2001, **118**, 99.
19 (*a*) C. P. Berlinguette, D. Vaughn, C. Canada-Vilalta, J. R. Galán-Mascarós and K. R. Dunbar, *Angew. Chem., Int. Ed.*, 2003, **42**, 1523; (*b*) W. Kaneko, S. Kitagawa and M. Ohba, *J. Am. Chem. Soc.*, 2007, **129**, 248; (*c*) J. Larionova, M. Gross, M. Pilkington, H. Andres, H. Stoeckli-Evans, H. U. Güdel and S. Decurtins, *Angew. Chem., Int. Ed.*, 2000, **39**, 1605.
20 (*a*) Y. -Z. Zheng, W. Xue, W.-X. Zhang, M.-L. Tong and X.-M. Chen, *Inorg. Chem.*, 2007, **46**, 6437; (*b*) R. P. John, M. Park, D. Moon, K. Lee, S. Hong, Y. Zou, C. S. Hong and M. Soo Lah, *J. Am. Chem. Soc.*, 2007, **129**, 14142; (*c*) G. Kong, G. N. Harakas and B. R. Whittlesey, *J. Am. Chem. Soc.*, 1995, **117**, 3502; (*d*) M. Wang, C. Ma, H. Wen and C. Chen, *Dalton Trans.*, 2009, 994.
21 (*a*) M. Manoli, R. D. L. Johnstone, S. Parsons, M. Murrie, M. Affronte, M. Evangelisti and E. K. Brechin, *Angew. Chem., Int. Ed.*, 2007, **46**, 4456; (*b*) M. Manoli, A. Collins, S. Parsons, A. Candini, M. Evangelisti and E. K. Brechin, *J. Am. Chem. Soc.*, 2008, **130**, 11129; (*c*) T. C. Stamatatos, K. A. Abboud, W. Wernsdorfer and G. Christou, *Angew. Chem., Int. Ed.*, 2006, **45**, 4134.
22 (*a*) L. P. Engelhardt, C. A. Muryn, R. G. Pritchard, G. A. Timco, F. Tuna and R. E. P. Winpenny, *Angew. Chem., Int. Ed.*, 2008, **47**, 924; (*b*) B. Hasenknopf, J.-M. Lehn, B. O. Kneisel, G. Baum and D. Fenske, *Angew. Chem., Int. Ed. Engl.*, 1996, **35**, 1838; (*c*) A. J. Stemmler, A. Barwinski, M. J. Baldwin, V. Young and V. L. Pecoraro, *J. Am. Chem. Soc.*, 1996, **118**, 11962; (*d*) C. S. Campos-Fernádez, R. Clérac, J. M. Koomen, D. H. Russell and K. R. Dunbar, *J. Am. Chem. Soc.*, 2001, **123**, 773; (*e*) O. Cador, D. Gatteschi, R. Sessoli, F. K. Larsen, J. Overgaard, A.-L. Barra, S. J. Teat, G. A. Timco and R. E. P. Winpenny, *Angew. Chem., Int. Ed.*, 2004, **43**, 5196; (*f*) H.-C. Yao, J.-J. Wang, Y.-S. Ma, O. Waldmann, W.-X. Du, Y. Song, Y.-Z. Li, L.-M. Zheng, S. Decurtins and X.-Q. Xin, *Chem. Commun.*, 2006, 1745.
23 (*a*) A. J. Tasiopoulos, W. Wernsdorfer, K. A. Abboud and G. Christou, *Inorg. Chem.*, 2005, **44**, 6324; (*b*) E. C. Sanudo, W. Wernsdorfer, K. A. Abboud and G. Christou, *Inorg. Chem.*, 2004, **43**, 4137; (*c*) T. C. Stamatatos, V. Nastopoulos, A. J. Tasiopoulos, E. E. Moushi, W. Wernsdorfer, G. Christou and S. P. Perlepes, *Inorg. Chem.*, 2008, **47**, 10081.
24 C. Lampropoulos, S. Hill and G. Christou, *ChemPhysChem*, 2009, **10**, 2397and references therein.